Future greenhouse gas emissions of automotive lithium-ion battery cell production

Xu, C.; Steubing, B.R.P.; Hu, M.; Harpprecht, C.I.; Meide, M.T. van der; Tukker, A.

Full length article

Future greenhouse gas emissions of automotive lithium-ion battery cell production

Chengjian Xu [a,*], Bernhard Steubing [a], Mingming Hu [a], Carina Harpprecht [a,b], Marc van der Meide [a], Arnold Tukker [a]

[a] *Institute of Environmental Sciences (CML), Leiden University, RA Leiden, 2300, The Netherlands*
[b] *German Aerospace Center (DLR), Institute of Networked Energy Systems, Curiestr. 4, 70563 Stuttgart, Germany*

A B S T R A C T

Understanding the future environmental impacts of lithium-ion batteries is crucial for a sustainable transition to electric vehicles. Here, we build a prospective life cycle assessment (pLCA) model for lithium-ion battery cell production for 8 battery chemistries and 3 production regions (China, US, and EU). The pLCA model includes scenarios for future life cycle inventory data for energy and key materials used in battery cell production. We find that greenhouse gas (GHG) emissions per kWh of lithium-ion battery cell production could be reduced from 41 to 89 kg CO_2-Eq in 2020 to 10–45 kg CO_2-Eq in 2050, mainly due to the effect of a low-carbon electricity transition. The Cathode is the biggest contributor (33%-70%) of cell GHG emissions in the period between 2020 and 2050. In 2050, LiOH will be the main contributor to GHG emissions of LFP cathodes, and Ni_2SO_4 for NCM/NCA cathodes. These results promote discussion on how to reduce battery GHG emissions.

1. Introduction

In the transportation sector, a global shift from internal combustion engine vehicles (ICEVs) to electric vehicles (EVs) has been widely recognized as one of the most effective ways to mitigate climate change (Kumar and Alok, 2020). The International Energy Agency (IEA) expects the global light-duty EV fleet to grow from around 10 million in 2021 to 124–199 million EVs in 2030 (IEA, 2022). Due to recent policy incentives and ongoing innovations in battery technologies and business models, amongst others, it is expected the global light-duty EV fleet size will grow to 970–1940 million EVs by 2050 (Xu et al., 2020).

The transition to the use of EVs will impact the supply chain of the automotive industry (Wells and Nieuwenhuis, 2012). One of the key changes exists in the production and use of batteries (Cano et al., 2018). Due to their low cost and high performance, lithium-ion batteries dominate the current EV market and are expected to dominate in the next decade. The most important battery types include lithium nickel cobalt manganese oxide batteries (NCM), lithium nickel cobalt aluminum oxide batteries (NCA), and lithium iron phosphate batteries (LFP).

Although a lot of studies have found that EVs have environmental advantages over ICEVs (Hawkins et al., 2013; Nordelöf et al., 2014;

Tagliaferri et al., 2016), the impacts of battery production are still rather uncertain (Ellingsen et al., 2014; Hiremath et al., 2015; Zackrisson et al., 2010). Current studies find quite diverging battery impacts (Ellingsen et al., 2017; Peters et al., 2017; Peters and Weil, 2018). This is due to the use of different data and assumptions on battery performance and compositions (Mohr et al., 2020), battery production processes, geographical scope (Kelly et al., 2020), and life cycle inventory (LCI) information (Ciez and Whitacre, 2019; Spangenberger et al., 2018), and environmental impact assessment methodologies (Schulz-Mönninghoff et al., 2021), amongst others. All these factors can lead to questionable conclusions on the magnitude of environmental impacts of battery production. Moreover, changes in environmental impacts of battery production in the next decades are rarely estimated, due to the challenges in estimating futurized background LCI data and modeling future battery production processes.

In this paper, we aim to overcome most of the aforementioned knowledge gaps by building a prospective life cycle assessment (pLCA) model to estimate future GHG emissions of the battery cell production per kWh battery capacity. The pLCA model simulates the lithium-ion battery cell production for 8 types of battery chemistries in 3 production regions (China, US, and EU) for the period 2020–2050. The foreground system is complemented by the prospective life cycle inventory

---

(pLCI) of background data that considers i) future energy scenarios as modeled in the Integrated Assessment Model REMIND (Baumstark et al., 2021) for the Shared Socio-Economic Pathway 2 (SSP2)-Base (no climate policy) and the SSP2-PkBudg 1100 scenarios (with climate policies)(2021) as well as ii) future supply chain of key battery metals including nickel, cobalt, copper, and others (see details in methods). In this way, this paper aims to contribute to a better understanding of the current and future GHG emissions of battery cell production and the

discussion of how to minimize such impacts in the context of a mobility transition towards EVs.

The paper is structured as follows. In section 2 we discuss the approach to the pLCA, discerning the goal and scope definition, life cycle inventory, and life cycle impact assessment. Section 3 gives the results and interpretation. Section 4 ends with discussions and conclusions.
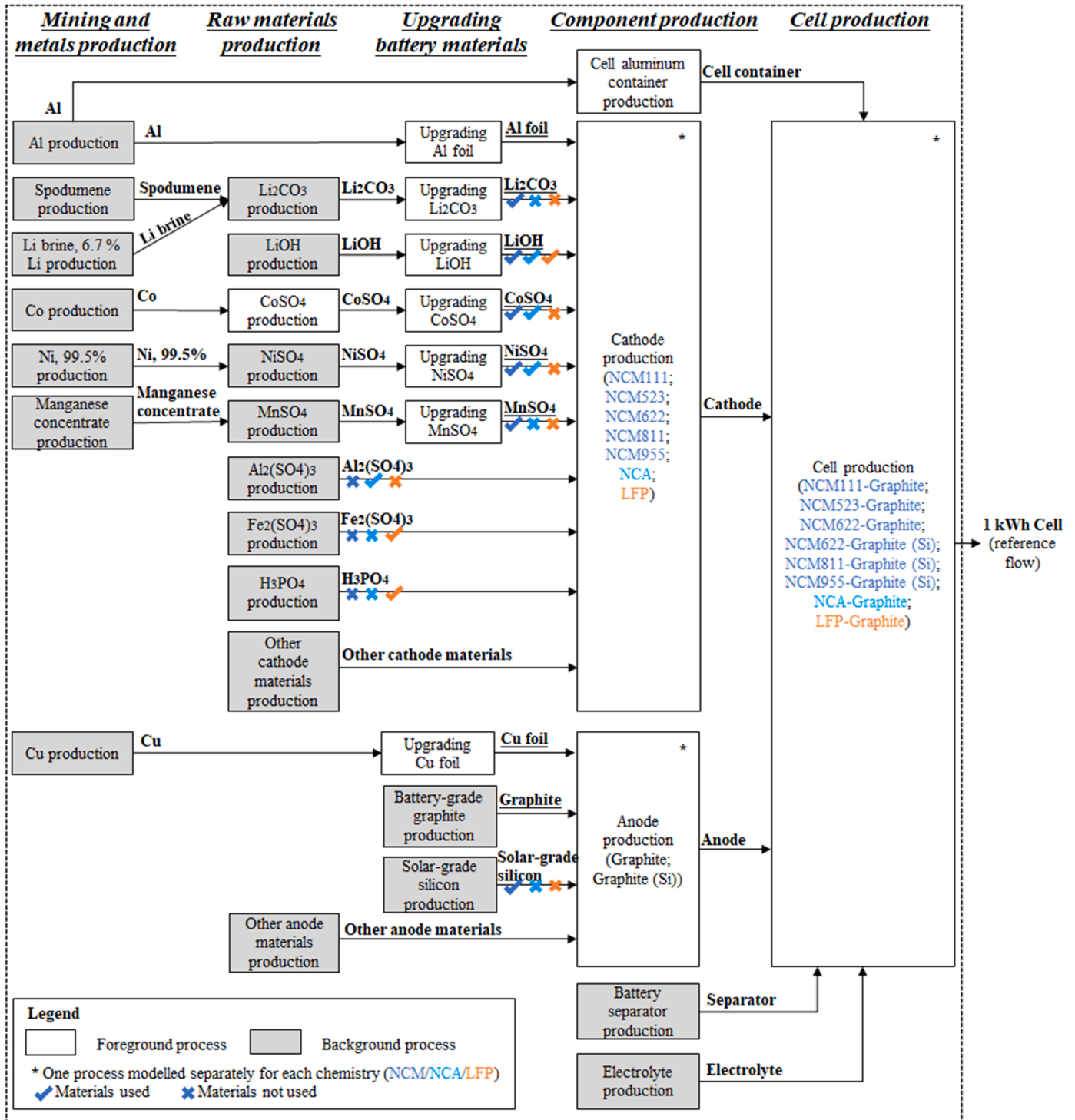
Fig. 1. Flowchart of the production of battery cells. Italicized underlined characters on top of the figure refer to life cycle stages. Materials with underlines indicate the quality of materials up to battery-grade, otherwise industry-grade.

2. Methods

2.1. Goal and scope

The goal of our pLCA model is to evaluate GHG emissions per kWh of battery cell production in 2020, 2030, 2040, and 2050. The modeled battery cell is a lithium-ion battery cell used in battery electric vehicles. The modeled cell capacity is 0.275 kWh, the most common size of an EV battery cell. The functional unit is chosen as 1 kWh in terms of the nominal battery cell capacity. The study is an attributional LCA, with a contribution analysis to reveal the environmental hotspots of battery cell production. The results are intended to give prospective environmental information to battery technology developers and EV policymakers.

The pLCA model covers 8 different battery chemistries and 3 production regions:

I. Battery chemistries. Battery chemistry development will lead to differences in material compositions and production processes and corresponding environmental impacts. Here we explore chemistry-specific GHG emissions by distinguishing 8 chemistries: LFP-Graphite, NCA-Graphite, NCM111-Graphite, NCM523-Graphite, NCM622-Graphite, NCM622-Graphite (Si), NCM811-Graphite (Si), and NCM955-Graphite (Si) batteries. We include these 8 chemistries because they are currently seen as the most likely dominant battery chemistries in the future according to our previous study (Xu et al., 2020).

II. Production regions. The battery production region determines where material and energy are supplied from, which significantly influences the associated environmental impacts. Here, we cover China, EU, and US as the main battery production regions in the world to explore region-specific GHG emissions.

Emissions of batteries in the use phase are negligible to zero. In the end-of-life phase, there may be benefits from 2nd uses or recycling of components or materials, but such scenarios and hence the environmental benefits of them are highly uncertain (Chengjian et al., 2022). We, therefore, apply cradle-to-gate system boundaries for this study which allocates all production impacts to the first use of the battery in an EV. We include the production of all battery cell components, *i.e.* cathode, anode, electrolyte, separator, and cell container, as well as the electric energy used to assemble all components into a complete cell (Fig. 1). We do not account for the environmental impacts of processing battery cells to battery modules and –packs, or other components such as battery management systems, as they are minor (less than 10% (Ellingsen et al., 2014)) compared to the battery cell production itself.

In the impact assessment, we focus on GHG emissions. We use the IPCC GWP 100 characterization method of 2013 that expresses GHG emissions in kg CO2-Eq. (Change, 2013). For the LCA implementation, we use the Activity Browser software (Steubing et al., 2020) to calculate the life cycle impacts for all battery chemistries, production regions, temporal boundary, and background scenarios.

2.2. Inventory analysis

2.2.1. Futurized background system

The futurized background system of our pLCA model is built based on the ecoinvent 3.6 database (Wernet et al., 2016), considering future energy scenarios and supply chains of key battery metals. Firstly, we use the premise (Sacchi et al., 2022) tool to build a futurized version of the ecoinvent 3.6 database (Wernet et al., 2016) (cut-off system model). The tool systematically builds regional LCIs of future electricity production based on detailed regional energy scenarios from the Integrated Assessment Model REMIND (Baumstark et al., 2021). Secondly, we incorporate technology scenarios for the future supply of key battery metals into the futurized version of the ecoinvent 3.6 database. Via this approach, we created the futurized background system of our pLCA model as follows.

I. Processes obtained from ecoinvent 3.6. We used ecoinvent 3.6 (Wernet et al., 2016) as a basis to build futurized LCIs of battery raw materials. From ecoinvent 3.6, we included Li_2Co_3, LiOH, $CoSO_4$, $NiSO_4$, $MnSO_4$, Al, and other materials for the production of the cathode. For the anode, we included graphite, silicon, Cu, and other materials. We further included all relevant raw materials and processes leading to the production of the separator, electrolyte, and cell container.

II. REMIND energy scenarios. We use the REMIND model (Baumstark et al., 2021) with Shared Socioeconomic Pathway 2 (SSP2) (O'Neill et al., 2014), a "middle-of-the-road" scenario with regard to future population and GDP growth. Under this SSP2 pathway, we use two future regional energy scenarios from REMIND model (Baumstark et al., 2021) to distinguish the effect of climate policy on the decarbonization of the electricity system. One is the "*SSP2-Base*" *scenario* where no specific climate policies are implemented and thus the global temperature could increase by more than 3.5 °Celsius by 2100. In the SSP2-Base scenario, the share of renewable energy (wind, solar, and hydro) will increase from only 24% in 2020 to 45% in 2050 for China, from 26% in 2020 to 63% in 2050 for EU, and from 14% 2020 to 54% in 2050 for US. The corresponding energy mix in 2050 will result in 0.4, 0.14, and 0.18 kg CO2-Eq per kWh electricity for China, EU, and US, respectively, reducing from 0.72, 0.36, and 0.48 kg CO2-Eq per kWh electricity in 2020. The second is the "*SSP2-PkBudg1100*" scenario, which has a goal to limit the cumulative global GHG emissions to 1100 gigatons by 2100, thus limiting the global average temperature increase to well below 2 °Celsius by 2100. In the SSP2-PkBudg1100 scenario, the share of renewable energy (wind, solar, and hydro) will further increase to 68%, 92%, and 93% for China, EU, and US in 2050, which leads to 0.079, 0.029, and 0.033 kg CO2-Eq per kWh electricity, respectively. Please see details in Supplementary Figs. 1 and 2 for regional energy mix and GHG emissions per kWh electricity production in 2020, 2030, 2040, and 2050.

III. Future technology scenarios for the supply of key battery metals. We incorporated the future technology supply scenarios of key battery metals as modeled by Harpprecht et al., (2021) and van der Meide et al., (2022) into the futurized version of the ecoinvent 3.6 database to create the background system. We consider future developments in the supply chains of the following key battery metals: copper (Harpprecht et al., 2021), nickel (Harpprecht et al., 2021), aluminum (International Aluminium Institute, 2020), lithium (Ambrose and Kendall, 2020a,b), and cobalt (van der Meide et al., 2022). These future supply chains use LCIs for the current situation as provided by ecoinvent 3.6 as a basis. For copper, we use the scenario developed by Harpprecht et al., (2021) to model future changes in ore grades, energy efficiency improvements, and market shares of primary and secondary production as well as of primary production routes. For nickel, we consider future ore grades and increased secondary production. For lithium, an increase of future secondary production share is assumed based on the work of[30,31]. For aluminum, future secondary production share will incresae based on the work of the International Aluminium Institute, (2020). We use the future cobalt supply chain developed by van der Meide et al., (2022). This model takes into account cobalt ore grade development, changes in the market shares of primary cobalt production routes, and changes in the share of secondary cobalt production share.

2.2.2. Battery cell production stages

In relation to the futurized background system, this section describes the battery cell production stages and relevant modeling choices, data sources, and assumptions. Battery cell production is taking place in five life cycle stages, namely: mining, raw materials production, upgrading battery materials, component production, and cell production (Fig. 1).

I. Mining and metals production. This life cycle stage refers to the extraction and concentration, smelting, refining, and other necessary procedures to produce metals. This stage includes the production processes of Al, spodumene, Li brine, Co, Ni (99.5%), manganese concentrate, and Cu for NCM cathodes; Al, spodumene, Li brine, Co, Ni

(99.5%), and Cu for NCA cathode; Al, spodumene, Li brine, and Cu for LFP cathode. The data source for this stage is the aforementioned futurized background system.

II. Raw materials production. Raw materials production refers to the production of raw materials from relevant metals, such as hydro-metallurgical leaching of Ni to produce $NiSO_4$. At this stage, the processes for producing Li_2CO_3, $LiOH$, $CoSO_4$, $NiSO_4$, $MnSO_4$, and other necessary battery raw materials are considered for NCM cathode; $LiOH$, $CoSO_4$, $NiSO_4$, $Al_2(SO4)_3$, and other necessary battery raw materials for NCA cathode; $LiOH$, $Fe_2(SO_4)_3$, H_3PO_4, and other necessary battery raw materials for LFP cathode. The data source for raw materials production is the aforementioned futurized background system, except for $CoSO_4$. We compile the LCIs for producing $CoSO_4$ from Co using information from the China battery industry reports in the period 2020–2022 (Eiafans, 2022).

III. Upgrading battery materials. The raw materials produced from the last life cycle stage are at the level of industrial-grade, which are not suitable for battery production yet. In this stage, raw materials are upgraded to a battery-grade level with additional materials and energy inputs. For the NCM cathode, this includes the production of battery-grade Li_2CO_3, battery-grade $LiOH$, battery-grade $CoSO_4$, battery-grade $NiSO_4$, battery-grade $MnSO_4$, and battery-grade Al; for the NCA cathode, battery-grade Li_2CO_3, battery-grade $LiOH$, battery-grade $CoSO_4$, battery-grade $NiSO_4$, and battery-grade Al foil are required; and for the LFP cathode battery-grade $LiOH$ is needed. For the anode production, we include the process for producing battery-grade Cu foil, battery-grade graphite, as well as solar-grade silicon if silicon is required for the anode (*i.e.* Graphite (Si) anode).

The LCI data for upgrading industrial-grade chemicals to battery-grade $LiOH$, battery-grade $CoSO_4$, and battery-grade $NiSO_4$ are based on the EverBatt model (Spangenberger et al., 2018) developed by Argonne National Laboratory to assess the cost and environmental impacts during the battery life cycle. The LCIs of battery-grade Li_2CO_3, battery-grade $MnSO_4$, battery-grade Al foil, and battery-grade Cu foil are compiled using information from the China battery industry reports (Eiafans, 2022).

IV. Component production. At the component production stage, the battery cell components, *i.e.* cathode, anode, electrolyte, separator, and cell container, are produced from battery-grade materials. From the EverBatt model (Spangenberger et al., 2018), we derive LCI data of cathode production from relevant battery-grade materials, including LFP, NCA, NCM111, NCM523, NCM622, and NCM811. These LCIs of cathode production are complemented by emissions inventory of nickel, cobalt, and manganese to air or water during cathode production (which is lost in the EverBatt model (Spangenberger et al., 2018)), using the information given in the China battery industry reports (Eiafans, 2022). In addition, we model the LCI of producing the NCM955 cathode based on that of the NCM811 cathode, based on their differences in material compositions.

V. Cell production. During this stage, all battery cell components are assembled into a complete cell. Our model for this stage considers material inputs and energy consumption. The material inputs are based on the composition of the battery cells as determined in the previous work of the authors (Xu et al., 2020). In cell production, electrical energy is used, and we need to account for the amount of electrical energy required to combine all battery components into a battery cell. There are only a few studies providing detailed energy consumption data for cell production, and they have large deviations (Erakca et al., 2021). The total energy consumption per Wh cell production is highly influenced by production volumes and could range from over 1000 Wh in the lab and pilot-scale to below 100 Wh on an industrial scale (Ellingsen et al., 2014). Here, we use an average electricity consumption from 5 industrial-scale studies, *i.e.* 74 Wh per Wh cell production (Erakca et al., 2021).

3. Results and interpretation

3.1. GHG emissions

Fig. 2 shows the cradle-to-gate GHG emissions for producing 1 kWh of cell capacity in 2020 by type of battery chemistry and production region. From the figure, we find a significant variation in the cradle-to-gate GHG emissions per kWh of battery cell production in China, US, and EU in 2020. This is mainly due to a substantial difference in the share of renewable energy and resulting emission intensities for electricity used for battery cell production across the three regions. In 2020, the EU electricity mix has the lowest emission intensity (0.36 kg CO2-Eq per kWh electricity), followed by the US (0.48 kg CO2-Eq per kWh electricity) and China (0.72 kg CO2-Eq per kWh electricity). As a consequence, the GHG emissions per kWh of battery cell produced in EU are 16%−18% lower than in the US, and 38%−41% lower than in China in 2020.

In addition to production regions, GHG emissions depend on battery chemistry as different materials and production processes are used. For instance, LFP does not require nickel, cobalt, and aluminum metals whose production is very energy-intensive and generates significant amounts of polluting emissions, while these metals are used for NCM and NCA cell production. For this reason, LFP cell production generates 20%−28% lower GHG emissions than NCA and NCM cells in terms of per kWh cell production, depending on the production region.

As a result, LFP cells produced in the EU can generate the lowest GHG emissions, while NCA and NCM cells produced in China can generate the highest emissions in 2020. There is a factor of ~2.2 between the lowest and highest GHG emissions per kWh of battery cell production in 2020.

3.2. Future GHG emissions

Given the similar GHG emissions of NCM and NCA chemistries, we show the future cradle-to-gate GHG emissions per kWh of battery cell production for two distinct chemistries in Fig. 3: LFP-Graphite cell and NCM622-Graphite cell (see results of other cell chemistries in Supplementary Figs. 3–5). Mainly due to the development of renewable and low-carbon electricity used for cell production, the cradle-to-gate GHG emissions of cell production per 1 kWh capacity is significantly reduced significantly from 2020 to 2050. Depending on battery chemistry and production region, the GHG emissions could be reduced by 49%−52% under the SSP2-Base scenario in 2020–2050, and even 74%−81% under the SSP2-PkBudg 1100 scenario during the same period.

In addition, the absolute variation in GHG emissions between production region and battery chemistry is expected to decline between 2020 and 2050. In 2020, the cradle-to-gate GHG emissions range from 41 to 89 (difference of 48) kg CO2-Eq per kWh battery cell capacity. In 2050, the cradle-to-gate GHG emissions range from 21 to 45 (difference of 24) kg CO2-Eq per kWh battery cell capacity in the SSP2-Base scenario and from 10 to 17 (difference of 7) kg CO2-Eq in SSP2-PkBudg 1100 scenario. Depending on energy scenarios, the corresponding absolute variation for GHG emissions in 2050 is 2–6.5 times lower than that in 2020.

3.3. Contribution analysis of battery cell

Figs. 2 and 3 also present the contribution of different cell components to GHG emissions results. The cathode, anode, and cell production[1] are the three most important contributors to GHG emissions. The relative contribution of the cathode for NCM/NCA cells is higher than that of LFP cells, while the relative contribution of the anode and cell production for LFP cells is higher than that of NCM/NCA cells. These are

---

[1] For cell production, only the impact of electricity used to assemble components into a cell is counted in our model.
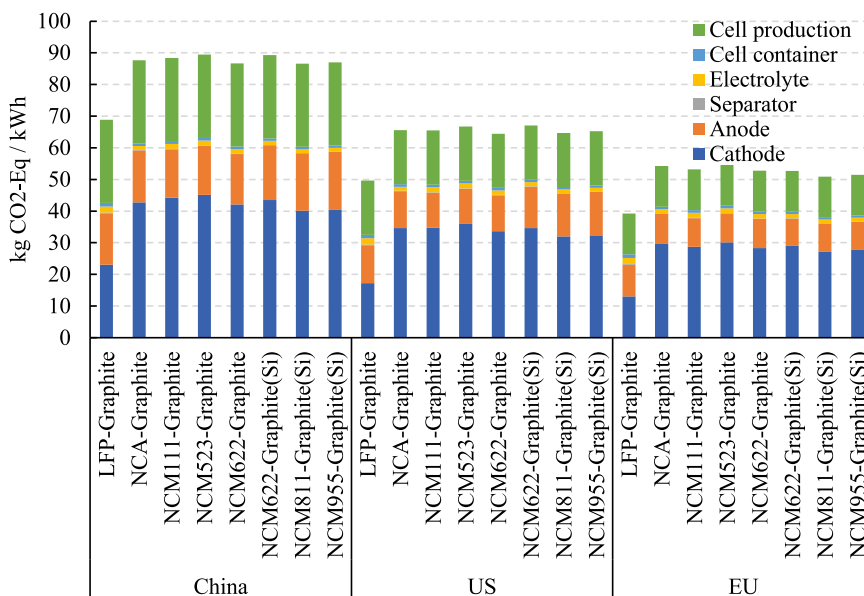
Fig. 2. Cradle-to-gate GHG emissions per kWh of cell production by battery chemistry and production region in 2020.
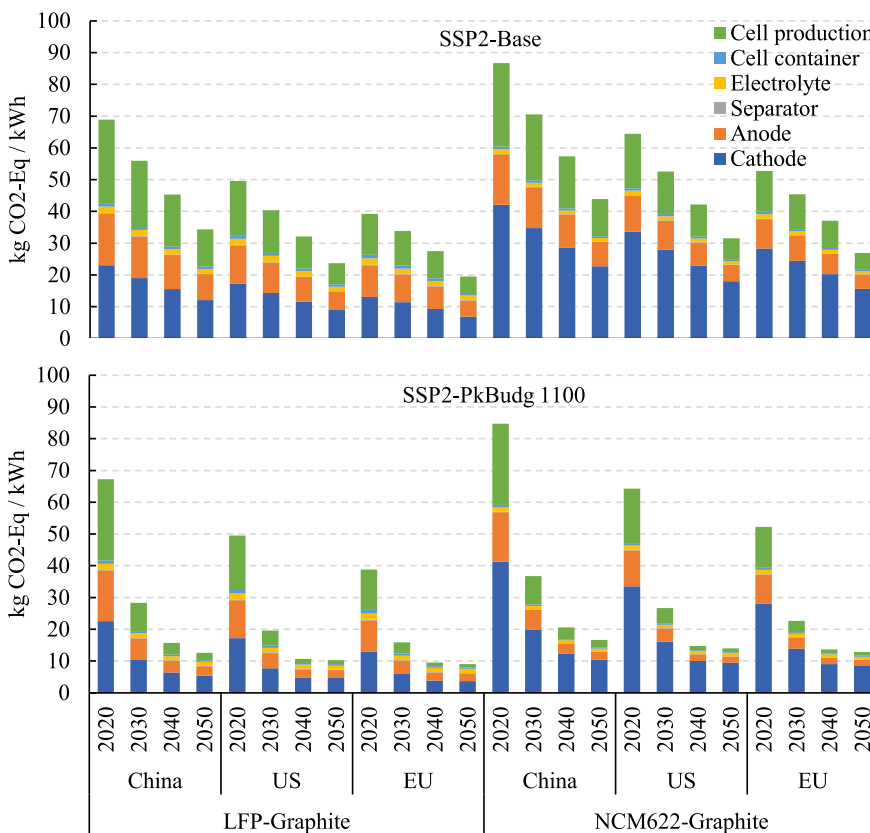

Fig. 3. Future GHG emissions per kWh of cell production for LFP-Graphite and NCM622-Graphite in China, EU, and US. Please see results for other cell chemistries in Supplementary Figs. 3–5.

mainly due to different material compositions between NCM/NCA cells and LFP cells.

The NCM/NCA cathode is, with 46%−55% depending on battery chemistry and production region, the biggest contributor to GHG emissions in 2020, which is more than the total contributions from all other components. This is because NCM/NCA cathodes make up around 53%−59% of the weight of battery cells and also its production relates to

the majority of metals contained in a battery cell which require GHG-intensive mining and refining processes (such as lithium, nickel, cobalt, and others). The NCM/NCA cathode is expected to remain the primary contributor to cradle-to-gate GHG emissions until 2050 (Fig. 3). Yet, its relative contribution is expected to increase to 49%−60% in the SSP2-Base scenario and 60%−70% in SSP2-PkBudg 1100 scenario during 2020–2050, depending on battery chemistry and production region.

Fig. 4 provides a relative contribution analysis by battery production life cycle stage. In 2020, the two most important life cycle stages from a GHG emissions perspective are "component production" followed by "cell production". They together account for 74%−83% of GHG emissions for LFP cells and 54%−69% for NCM/NCA cells, depending on production region/cell chemistry. These numbers could decrease to 39%−76% for LFP cells and 23%−61% for NCM/NCA cells depending on energy scenarios, due to the stronger effects of low-carbon energy development on life cycle stages of "cell production" and component production" rather than other life cycle stages.

"Mining and metals production" could become a significant life cycle stage for NCM/NCA cells in the future, especially when considering a stronger low-carbon energy development scenario. The SSP2-PkBudg 1100 scenario could result in "mining and metals production" as the primary life cycle stage of GHG emissions, accounting for 33%−42% of NCA cells and 24%−47% of NCM cells in 2050. Note that for NCM cells, the future transition from NCM111 chemistry to NCM955 chemistry will improve the contribution of "mining and metals production" to GHG emissions. This transition increases the content of Ni with relatively high GHG emissions (7 kg CO2-Eq in 2020 and 3–4.7 kg CO2-Eq in 2050 per kg $NiSO_4$ globally) and decreases the content of Co with relatively low GHG emissions (2.7 kg CO2-Eq in 2020 and 1.2–1.7 kg CO2-Eq in 2050 per kg $CoSO_4$ globally) for NCM cells, resulting in an overall increase in GHG emission during the life cycle stage of "mining and metals production".

3.4. Contribution analysis of cathode

Given the substantial contribution of the cathode in the battery GHG emissions, we perform an absolute contribution analysis for cathode disaggregated by life cycle stage, with each stage divided into energy and materials input. Fig. 5 presents the results for LFP and NCM622 cathodes produced in China in 2020 and 2050 (please see the results of US and EU in Supplementary Figs. 6 and 7). The contribution analysis results differ a lot between LFP and NCM622 cathodes. For battery cells produced in China in 2020, the life cycle stage of "mining and metals production" and "cathode production" contributes to around 22% and 44% for NCM622 cathode respectively, while these numbers are 2% and 71% for LFP cathode.

In addition, the energy input dominates (around 78%) the cradle-to-gate GHG emissions of the LFP cathode, while the energy input and materials have almost equal contributions to GHG emissions for the NCM622 cathode in 2020. In the future, input materials, rather than input energy, will become more important contributors to GHG emissions due to the decarbonization of the electricity system. Input materials will even become the major source of cradle-to-gate GHG emissions for cathodes in 2050, with a relative contribution of up to 34%−81% for LFP cathodes and 52%−71% for NCM/NCA cathodes depending on
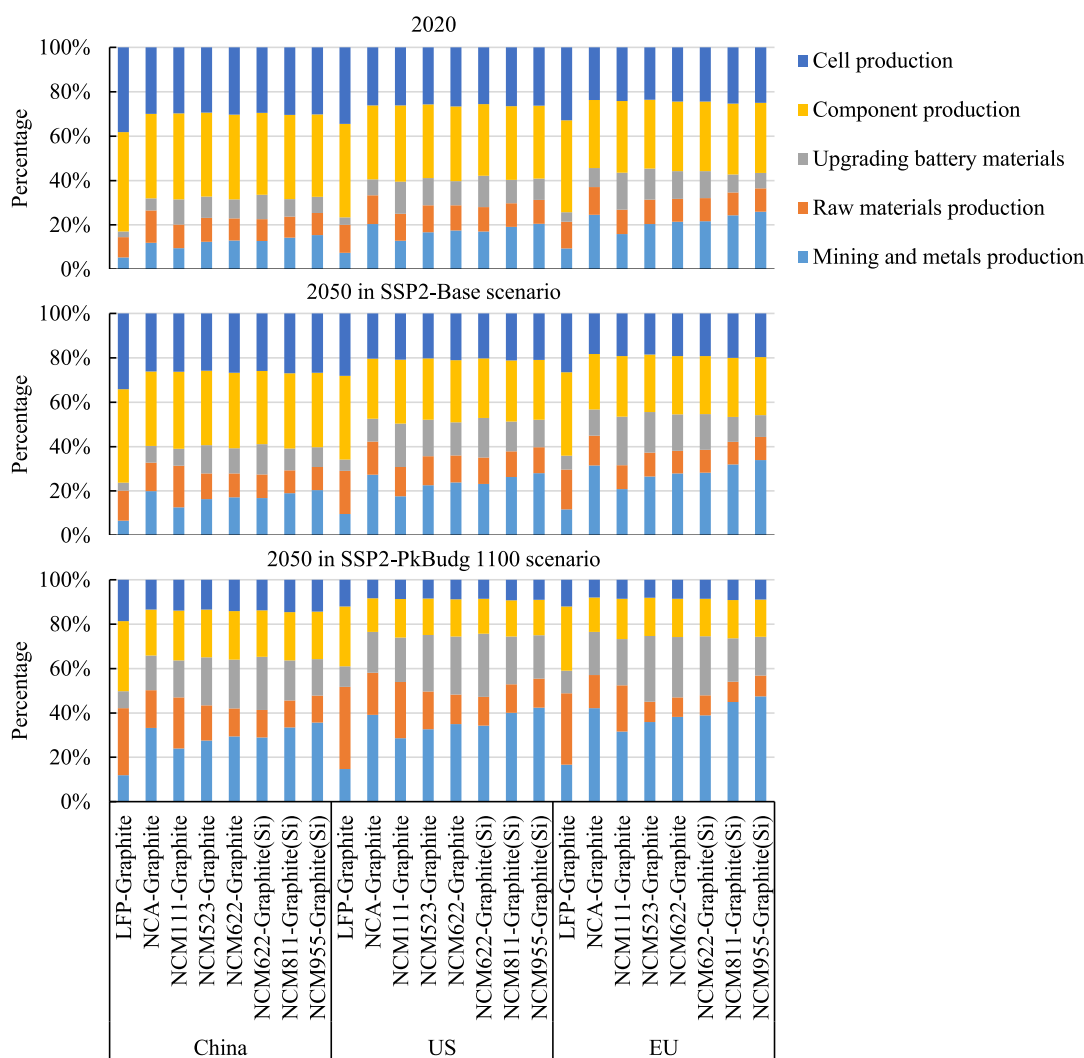

Fig. 4. GHG emission contributions by life cycle stage for different battery cell chemistries and production regions in 2020 and 2050.
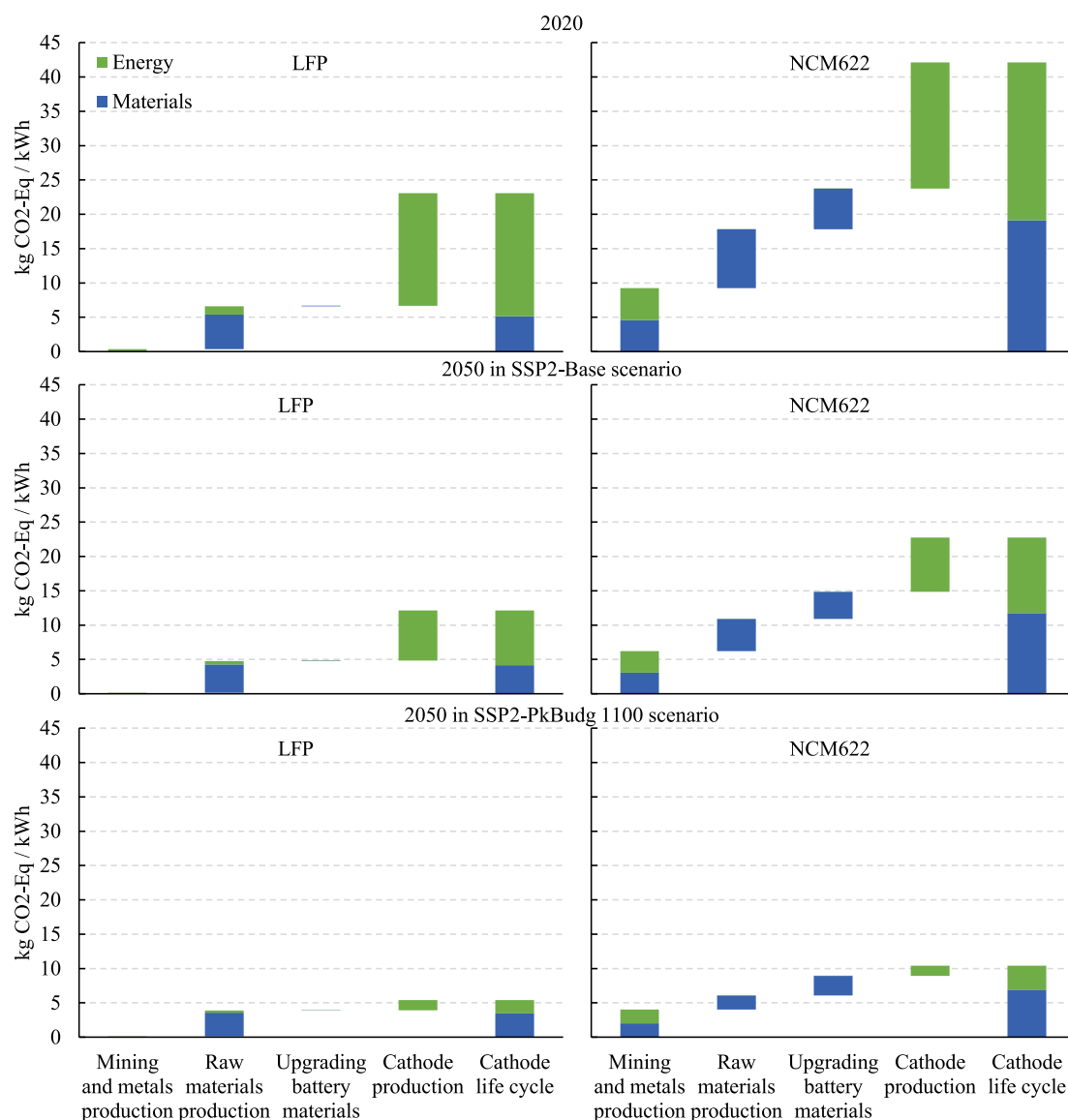
Fig. 5. Absolute contribution analysis of cradle-to-gate GHG emission of the cathode production for 1 kWh battery cell capacity by life cycle stages, divided by input energy and input materials, for LFP and NCM622-Graphite in China in 2020 and 2050. Please see results of US and EU in Supplementary Figs. 6 and 7.

energy scenarios/production regions/cell chemistries.

[Fig. 6](#) further illustrates which specific materials and energy sources account for the GHG emissions for LFP and NCM622 cathodes. LiOH and electricity are key contributors to the GHG emission of LFP cathodes. They together account for 82–86% in 2020 and 64%–82% in 2050 of GHG emissions for LFP cathodes, depending on the production region. Taking the perspective of the production of the whole LFP cell, LiOH and electricity together contribute to 27%–29% in 2020 and 28%–35% in 2050 of GHG emissions for the production of LFP cells.

Looking at the cradle-to-gate GHG emissions of NCM622 cathode production, $NiSO_4$ and Li_2CO_3 materials, rather than $CoSO_4$ and other cathode materials, are important contributors. $NiSO_4$ and Li_2CO_3 can contribute to 18%−30% and 6%−11% of GHG emissions of NCM622 cathode in 2020 respectively. These numbers change to 25%−46% and 8%−21% in 2050, depending on the production region and energy scenarios. In other words, $NiSO_4$ and Li_2CO_3 can account for 16%−31% and 5%−14% of GHG emissions of NCM622 cells in 2050.

4. Discussion

In this study, we build a prospective LCA model to quantify future cradle-to-gate GHG emissions per kWh battery cell production for 8 types of cell chemistries and 3 production regions until 2050. According to the pLCA model, our results for GHG emissions per kWh battery cell production (53–85 kg CO2-Eq per kWh in 2020 and 10–45 kg CO2-Eq per kWh in 2050) lie in the lower end of the range of earlier studies found in literatures ([Bouter and Guichet, 2022](#); [Ciez and Whitacre, 2019](#); [Peters et al., 2017](#)) (28–356 kg CO2-Eq per kWh). However, our results compare well with the findings from the International Council of Clean Transportation ([Bieker, 2021](#)) (34–77 kg CO2-Eq per kWh in 2021). There are various explanations for this. First, existing literature uses dated LCI data for battery cell production. Our modeling uses up-to-date LCI data based on the EverBatt model ([Spangenberger et al., 2018](#)) and China battery industry reports in the period 2020–2022 ([Eiafans, 2022](#)), which takes changes in battery chemistry next to cell production into account. Second, we take into account the effects of the low-carbon energy transition on battery production based on the integrated assessment model REMIND. Results are intended to give reliable insights
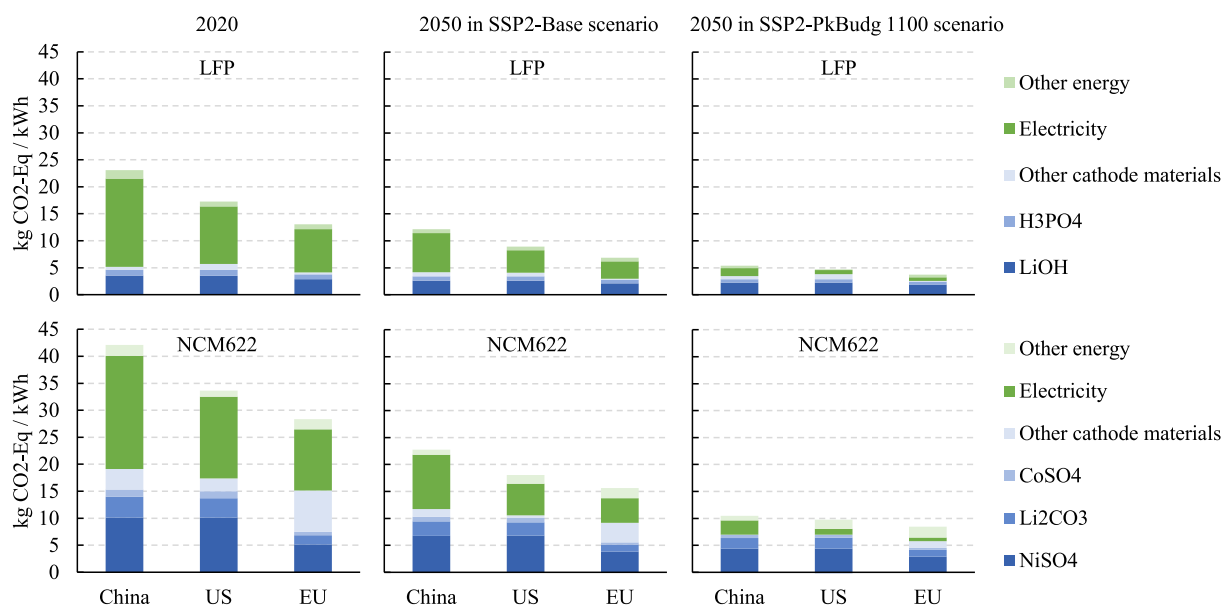
Fig. 6. Absolute contribution analysis of GHG emissions of the cathode production split by materials and energy, in terms of 1 kWh battery cell capacity.

into future cradle-to-gate GHG emissions from battery cell production, which can form a basis for suggestions to further reduce impacts from this production.

Since LFP battery is expected to generate less GHG emissions than NCM/NCA batteries until 2050, one option is to support LFP battery deployment. The somewhat lower specific energy (Wh/kg) of LFP batteries compared to NCM/NCA batteries may be an obstacle to the large-scale deployment of LFP batteries. At the same time, the advantages of LFP batteries are their relatively long useful lifetimes and the low material cost of LFP batteries. Battery producers can take advantage of this, and at the same time invest in improving LFP battery performance. One example is that several battery producers started to improve the mass and space utilization of the battery pack by removing modules and directly assembling cells into a pack (the LFP blade battery created by BYD can reach the specific energy of 140 Wh/kg at the pack level, which is higher than that of a standard NMC622 prismatic battery) (Yang et al., 2021).

Choosing battery production regions, which determines the electricity mix used to produce batteries, could be another important factor to consider for battery producers to reduce GHG emissions. China dominates the battery production market and is expected to continue so in the next decade. Reducing the emissions of China's electricity supply is key to achieving a lower GHG impact. EU and US provide greener electricity supply than China, and in theory, they are ideal regions for producing batteries with the lowest GHG emissions. However, it may not be possible to put a complete battery production supply chain in EU and US in the short term due to an uneven geographical distribution of extraction locations for primary materials required for batteries. Putting some part of the battery production life cycle stages in EU or US, rather than China, can be a pathway to start reducing the impacts of battery production. This could be particularly considered for energy-intensive production stages such as cell production which uses electric energy to assemble all battery components into a complete cell.

We must emphasize the crucial role of a low-carbon electricity transition in reducing GHG emissions of battery production, as reflected by the results of the SSP2-PkBudg 1100 scenario. The energy supply for battery production should be as carbon-neutral as possible. For instance, Tesla's announced Giga watt-hour battery production factory is planned to be built together with a solar energy supply facility (Tesla, 2022). In this case, a 100% supply of solar power for battery production is ensured, which can lead to extremely low GHG emissions.

Given the major contribution of the use of $NiSO_4$ and Li_2CO_3 to the GHG emissions of the production of NCM/NCA batteries and of the use of LiOH to GHG of LFP batteries, the reduction of GHG emissions along the supply chain of Ni and Li metals is relevant too. Replacing fossil fuels with renewable electricity, improving energy efficiency, as well as controlling and capturing the GHG emissions during nickel mining and refining can be effective ways to reduce the impacts of $NiSO_4$ production. We can apply the sameways to Li. Moreover, Li_2CO_3 produced from the leaching of spodumene with sulfuric acid can generate less emissions than when it is produced from concentrated brine (Kelly et al., 2021). The spodumene leaching pathway has currently still a minor market share of the Li_2CO_3 production market. Promoting this pathway is another option to reduce GHG emissions related to LFP battery production.

There are some future developments, which we did not consider in this study. Firstly, although we included a wide range of scenarios for battery chemistries, metal production, and energy generation, other scenarios may play out in the future (*e.g.* deeper decarbonization of the energy system, or low-impact production processes for certain materials, such as the application of inert anodes in the Hall-Herault process for aluminum production (Ratvik et al., 2022). Secondly, it is possible that the expected fast scaling up to high-volume production of the batteries considered in this study leads to considerable learning effects. This can result in significant efficiency improvements and lower costs and impacts, for instance by using automated manufacturing technologies using robots (Tilley, 2017). Thirdly, the development of new break-through battery technologies, such as solid-state Lithium-Sulphur and Lithium-Air batteries (Manthiram et al., 2017), Na-ion (European et al., 2020), etc., may create radical changes in battery production processes and relevant materials supply chains. It is currently unclear if such technologies indeed will break through. There is further insufficient experience with such novel battery technologies to make a reliable quantitative estimate of life cycle inventory data, while also little is known about the impacts of such novel battery technologies once they have been scaled up from lab or pilot scale to full production plants.

CRediT authorship contribution statement

Chengjian Xu: Conceptualization, Methodology, Investigation, Formal analysis, Writing – original draft, Visualization. **Bernhard Steubing:** Conceptualization, Writing – review & editing. **Mingming**

Data availability

Data will be made available on request.

Supplementary materials

Supplementary material associated with this article can be found, in the online version, at doi:10.1016/j.resconrec.2022.106606.

References

Ambrose, H., Kendall, A., 2020a. Understanding the future of lithium: part 1, resource model. J. Ind. Ecol. 24 (1), 80–89.

Ambrose, H., Kendall, A., 2020b. Understanding the future of lithium: part 2, temporally and spatially resolved life-cycle assessment modeling. J. Ind. Ecol. 24 (1), 90–100.

Baumstark, L., Bauer, N., Benke, F., Bertram, C., Bi, S., Gong, C.C., Dietrich, J.P., Dirnaichner, A., Giannousakis, A., Hilaire, J., Klein, D., Koch, J., Leimbach, M., Levesque, A., Madeddu, S., Malik, A., Merfort, A., Merfort, L., Odenweller, A., Pehl, M., Pietzcker, R.C., Piontek, F., Rauner, S., Rodrigues, R., Rottoli, M., Schreyer, F., Schultes, A., Soergel, B., Soergel, D., Strefler, J., Ueckerdt, F., Kriegler, E., Luderer, G., 2021. REMIND2.1: transformation and innovation dynamics of the energy-economic system within climate and sustainability limits. Geosci. Model Dev. 14 (10), 6571–6603.

Bieker, G., 2021. A global comparison of the life-cycle greenhouse gas emissions of combustion engine and electric passenger cars. Communications 49, 847129-847102.

Bouter, A., Guichet, X., 2022. The greenhouse gas emissions of automotive lithium-ion batteries: a statistical review of life cycle assessment studies. J. Clean. Prod., 130994

Cano, Z.P., Banham, D., Ye, S., Hintennach, A., Lu, J., Fowler, M., Chen, Z., 2018. Batteries and fuel cells for emerging electric vehicle markets. Nat. Energy 3 (4), 279–289.

Change, I.C., 2013. The Physical Science Basis. Cambridge Univ. Press.

Chengjian, X., Paul, B., Paul, G., Kandler, S., Mingming, H., Arnold, T., Bernhard, S., 2022. Electric vehicle batteries alone could satisfy short-term grid storage demand by as early as 2030. *Submitted to* Nat. Commun.

Ciez, R.E., Whitacre, J.F., 2019. Examining different recycling processes for lithium-ion batteries. Nat. Sustain. 2 (2), 148–156.

Eiafans, 2022. Environmental impact assessment reports in China. http://www.eiafans.com/forum.php.

Ellingsen, L.A.-W., Hung, C.R., Strømman, A.H., 2017. Identifying key assumptions and differences in life cycle assessment studies of lithium-ion traction batteries with focus on greenhouse gas emissions. Transp. Res. Part D: Transp. Environ. 55, 82–90.

Ellingsen, L.A.-W., Majeau-Bettez, G., Singh, B., Srivastava, A.K., Valøen, L.O., Strømman, A.H., 2014. Life cycle assessment of a lithium-ion battery vehicle pack. J. Ind. Ecol. 18 (1), 113–124.

Erakca, M., Baumann, M., Bauer, W., de Biasi, L., Hofmann, J., Bold, B., Weil, M., 2021. Energy flow analysis of laboratory scale lithium-ion battery cell production. iScience 24 (5), 102437.

European, C., Directorate-General for Climate, A., Hill, N., Amaral, S., Morgan-Price, S., Nokes, T., Bates, J., Helms, H., Fehrenbach, H., Biemann, K., Abdalla, N., Jöhrens, J., Cotton, E., German, L., Harris, A., Haye, S., Sim, C., Bauen, A., Ziem-Milojevic, S., 2020. Determining the Environmental Impacts of Conventional and Alternatively Fuelled Vehicles Through LCA : Final Report. Publications Office.

Harpprecht, C., van Oers, L., Northey, S.A., Yang, Y., Steubing, B., 2021. Environmental impacts of key metals' supply and low-carbon technologies are likely to decrease in the future. J. Ind. Ecol. 25 (6), 1543–1559.

Hawkins, T.R., Singh, B., Majeau-Bettez, G., Strømman, A.H., 2013. Comparative environmental life cycle assessment of conventional and electric vehicles. J. Ind. Ecol. 17 (1), 53–64.

Hiremath, M., Derendorf, K., Vogt, T., 2015. Comparative life cycle assessment of battery storage systems for stationary applications. Environ. Sci. Technol. 49 (8), 4825–4833.

IEA, 2022. Global EV Outlook 2022. International Energy Agency, Paris, France.

Kelly, J.C., Dai, Q., Wang, M., 2020. Globally regional life cycle analysis of automotive lithium-ion nickel manganese cobalt batteries. Mitigation and Adaptation Strategies for Glob. Change 25 (3), 371–396.

Kelly, J.C., Wang, M., Dai, Q., Winjobi, O., 2021. Energy, greenhouse gas, and water life cycle analysis of lithium carbonate and lithium hydroxide monohydrate from brine and ore resources and their use in lithium ion battery cathodes and lithium ion batteries. Resour. Conserv. Recycl. 174, 105762.

Kumar, R.R., Alok, K., 2020. Adoption of electric vehicle: a literature review and prospects for sustainability. J. Clean. Prod. 253, 119911.

Manthiram, A., Yu, X., Wang, S., 2017. Lithium battery chemistries enabled by solid-state electrolytes. Nat. Rev. Mater. 2 (4), 16103.

Mohr, M., Peters, J.F., Baumann, M., Weil, M., 2020. Toward a cell-chemistry specific life cycle assessment of lithium-ion battery recycling processes. J. Ind. Ecol. 24 (6), 1310–1322.

Nordelöf, A., Messagie, M., Tillman, A.-.M., Ljunggren Söderman, M., Van Mierlo, J., 2014. Environmental impacts of hybrid, plug-in hybrid, and battery electric vehicles—What can we learn from life cycle assessment? Int. J. Life Cycle Assess. 19 (11), 1866–1890.

O'Neill, B.C., Kriegler, E., Riahi, K., Ebi, K.L., Hallegatte, S., Carter, T.R., Mathur, R., van Vuuren, D.P., 2014. A new scenario framework for climate change research: the concept of shared socioeconomic pathways. Clim. Change 122 (3), 387–400.

Peters, J.F., Baumann, M., Zimmermann, B., Braun, J., Weil, M., 2017. The environmental impact of Li-Ion batteries and the role of key parameters – A review. Renew. Sustain. Energy Rev. 67, 491–506.

Peters, J.F., Weil, M., 2018. Providing a common base for life cycle assessments of Li-Ion batteries. J. Clean. Prod. 171, 704–713.

International Aluminium Institute, 2020. GLOBAL ALUMINIUM CYCLE 2019. https://alucycle.world-aluminium.org/public/global/index.html.

Ratvik, A.P., Mollaabbasi, R., Alamdari, H., 2022. Aluminium production process: from Hall–Héroult to modern smelters. ChemTexts 8 (2), 10.

Sacchi, R., Terlouw, T., Siala, K., Dirnaichner, A., Bauer, C., Cox, B., Mutel, C., Daioglou, V., Luderer, G., 2022. PRospective EnvironMental Impact asSEment (premise): a streamlined approach to producing databases for prospective life cycle assessment using integrated assessment models. Renew. Sustain. Energy Rev. 160, 112311.

Schulz-Mönninghoff, M., Bey, N., Nørregaard, P.U., Niero, M., 2021. Integration of energy flow modelling in life cycle assessment of electric vehicle battery repurposing: evaluation of multi-use cases and comparison of circular business models. Resour. Conserv. Recycl. 174, 105773.

Spangenberger, J., Gaines, L., Dai, Q., 2018. Recell; a closed-loop battery recycling model. ECS Meeting Abstracts MA2018-01 (4), 616-616.

Steubing, B., de Koning, D., Haas, A., Mutel, C.L., 2020. The activity browser — an open source LCA software building on top of the brightway framework. Software Impacts 3, 100012.

Tagliaferri, C., Evangelisti, S., Acconcia, F., Domenech, T., Ekins, P., Barletta, D., Lettieri, P., 2016. Life cycle assessment of future electric and hybrid vehicles: a cradle-to-grave systems engineering approach. Chem. Eng. Res. Design 112, 298–309.

Tesla, 2022. Tesla Gigafactory 2. https://www.tesla.com/gigafactory.

Tilley, J., 2017. Automation, robotics, and the factory of the future. McKinsey mckinsey.com/business-functions/operations/our-insights/automation-robotics-and-the-factory-of-the-future.

van der Meide, M., Harpprecht, C., Northey, S., Yang, Y., Steubing, B., 2022. Effects of the energy transition on environmental impacts of cobalt supply: a prospective life cycle assessment study on future supply of cobalt. J. Ind. Ecol. n/a(n/a).

Wells, P., Nieuwenhuis, P., 2012. Transition failure: understanding continuity in the automotive industry. Technol. Forecast. Soc. Change 79 (9), 1681–1692.

Wernet, G., Bauer, C., Steubing, B., Reinhard, J., Moreno-Ruiz, E., Weidema, B., 2016. The ecoinvent database version 3 (part I): overview and methodology. Int. J. Life Cycle Assess. 21 (9), 1218–1230.

Xu, C., Dai, Q., Gaines, L., Hu, M., Tukker, A., Steubing, B., 2020. Future material demand for automotive lithium-based batteries. Commun. Mater. 1 (1), 99.

Yang, X.-.G., Liu, T., Wang, C.-.Y., 2021. Thermally modulated lithium iron phosphate batteries for mass-market electric vehicles. Nat. Energy 6 (2), 176–185.

Zackrisson, M., Avellán, L., Orlenius, J., 2010. Life cycle assessment of lithium-ion batteries for plug-in hybrid electric vehicles – Critical issues. J. Clean. Prod. 18 (15), 1519–1529.